

---

This is an electronic reprint of the original article.  
This reprint may differ from the original in pagination and typographic detail.

Herrala, Reima; Wang, Zulin; Vapaavuori, Jaana; Lundström, Mari; Yliniemi, Kirsi  
**Recovery of Gold as Nanoparticles from Gold-Poor Au-Cu-Cl Solutions**

*Published in:*  
Journal of Physical Chemistry C

*DOI:*  
[10.1021/acs.jpcc.3c03135](https://doi.org/10.1021/acs.jpcc.3c03135)

Published: 17/08/2023

*Document Version*  
Publisher's PDF, also known as Version of record

*Published under the following license:*  
CC BY

*Please cite the original version:*  
Herrala, R., Wang, Z., Vapaavuori, J., Lundström, M., & Yliniemi, K. (2023). Recovery of Gold as Nanoparticles from Gold-Poor Au-Cu-Cl Solutions. *Journal of Physical Chemistry C*, 127(32), 16099–16109.  
<https://doi.org/10.1021/acs.jpcc.3c03135>

---

This material is protected by copyright and other intellectual property rights, and duplication or sale of all or part of any of the repository collections is not permitted, except that material may be duplicated by you for your research use or educational purposes in electronic or print form. You must obtain permission for any other use. Electronic or print copies may not be offered, whether for sale or otherwise to anyone who is not an authorised user.

# Recovery of Gold as Nanoparticles from Gold-Poor Au-Cu-Cl Solutions

Reima Herrala, Zulin Wang, Jaana Vapaavuori, Mari Lundström, and Kirsi Yliniemi\*



Cite This: *J. Phys. Chem. C* 2023, 127, 16099–16109



Read Online

ACCESS |



Metrics & More

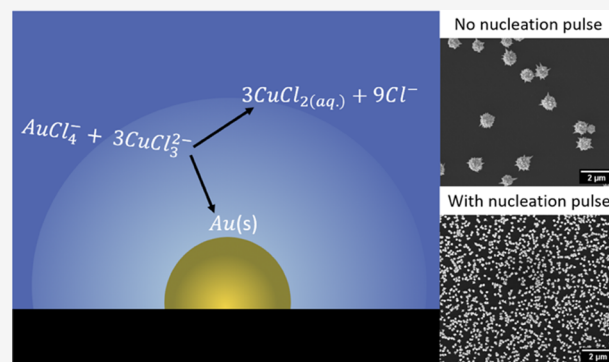


Article Recommendations



Supporting Information

**ABSTRACT:** Electrochemical methods for preparing functional surfaces typically use optimized solutions where competing reactions do not need to be considered. However, with the increased demand for resource efficiency, selective deposition methods that can make use of more complex solutions are gaining importance. In this study, we show how gold recovery as nanoparticles from Au-Cu-Cl solutions can be assisted by electrochemically generated  $\text{Cu}^{1+}$  species. In the electrochemically assisted reduction (EAR) method, a low-energy electrochemical step is employed, followed by spontaneous gold reduction onto the electrode. The studied solutions mimic challenging hydrometallurgical process solutions where the ratio of gold (5 ppm) to copper (20 g/L) is low. In addition to selective gold recovery, by controlling the electrochemical pulse parameters, the loss of deposits due to corrosion could be minimized, current efficiency improved from  $\sim 0$  to  $>10\%$ , and relatively narrow particle size distributions achieved ( $43 \pm 10$  nm), and this can be done even at a high (4.5 M) NaCl concentration.



## INTRODUCTION

More efficient utilization of existing resources is a key component of sustainable development.<sup>1</sup> With the increased availability of renewable energy,<sup>2</sup> replacing existing metal recovery methods with electrically driven rather than chemical-heavy processes may reduce their environmental burden. Thus, electrochemical processes, where metals are reduced out of solution through an applied current, will become more attractive for recovery. However, selective and effective recovery of critical and/or valuable metals from hydrometallurgical solutions can be challenging when their concentration is low relative to other metals present.

In hydrometallurgy, chloride solutions can be used for the leaching of both primary and secondary metal-containing raw materials.<sup>3–5</sup> In particular, leaching gold with copper chloride has been studied<sup>6,7</sup> as a less toxic alternative to traditional cyanide leaching. Since gold and copper are often found together in ores in varying ratios,<sup>8</sup> the capability of chloride to effectively leach copper ores increases the utilization potential of this method on industrial scale.<sup>9,10</sup> Due to the variation in raw material, the gold concentration may often be too low for its viable recovery. However, value may be found by using a single recovery step to directly create a functional surface, as gold can be deposited electrochemically as nanoparticles,<sup>11,12</sup> which have found applications especially in catalysis<sup>13–16</sup> and chemical sensing.<sup>17–21</sup> Compared to producing bulk metals, nanostructures typically require relatively low amounts of metal and therefore may be able to better take advantage of resource streams where the concentrations are low.

The electrochemical approach for nanoparticle synthesis allows dynamic control of morphology by varying parameters such as deposition potential, current density, and pulsing behavior.<sup>22–25</sup> This can be advantageous, as the size of these particles is often critical for functionality in part due to the increased surface area. Furthermore, if these nanoparticles can be produced electrochemically from existing solutions in industry, then some of the environmental burden from synthesis can be avoided.

A recently developed electrochemical method to recover noble metals from solutions with large differences in concentration is electrodeposition-redox replacement (EDRR).<sup>26</sup> In EDRR, a sacrificial layer is first electrodeposited (typically using a metal that is abundant in the solution), after which a spontaneous replacement reduction occurs between the dissolved noble metals (also present at low concentration) in the solution and the deposited layer. In a recent publication studying the EDRR method for copper and gold in chloride solutions, Korolev et al.<sup>27</sup> noted that spontaneous corrosion of deposited copper (eq 1) was followed by an aqueous

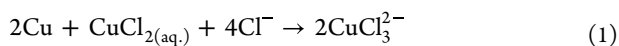
Received: May 12, 2023

Revised: July 17, 2023

Published: August 4, 2023

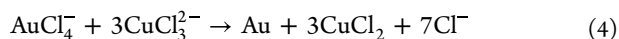


cementation reaction between the dissolved aurous and cuprous species (eq 2), resulting in additional gold deposition.



The key difference in the method used by Korolev et al. to traditional gold cementation<sup>28,29</sup> is the use of a direct electrochemical approach to create a reductant, either as solid copper (EDRR) or as aqueous cuprous chloride near the electrode.

In this work, for the first time, we have studied the aqueous reduction approach to recover gold as nanoparticles, with the aim of directly preparing functional surfaces from gold-poor Au-Cu-Cl solutions. Unlike in the work by Korolev et al.,<sup>27</sup> the reductant ( $\text{Cu}^{+1}$ ) for gold recovery is generated electrochemically according to eq 3. This approach is hereafter referred to as electrochemically assisted aqueous reduction (EAR). In addition, trivalent  $\text{Au}^{3+}$  is used, according to eq 4. In real solutions, the oxidation state of gold varies based on the leaching process. For example, gold has been reported to leach primarily as  $\text{AuCl}_4^-$  by chlorine,<sup>30</sup> while leaching by cupric chloride<sup>31</sup> produced  $\text{AuCl}_2^-$ .



It is expected that since EAR operates at a more positive potential than EDRR and no solid sacrificial layer is deposited, the purity of the resulting surface is higher. Despite both reactants being in the solution phase, it is expected that gold would accumulate onto the electrode due to the generally lower energy requirement of heterogeneous nucleation compared to homogeneous nucleation within the solution.<sup>32</sup> The possible downside of the reductant not being attached to the electrode surface is that it will migrate away before reacting with gold, and consequently the current efficiency may be affected.

In chloride solutions, both cuprous ( $\text{Cu}^{+1}$ ) and cupric ( $\text{Cu}^{+2}$ ) species are stable, which is essential for this process. With increasing chloride concentration, the cuprous chlorides become more stable,<sup>33,34</sup> which increases the reduction potential of cupric chloride solutions and is therefore expected to affect the driving force of the EAR process (eqs 2 and 4).

Here, we systematically demonstrate that EAR can be used to recover gold as nanoparticles from copper chloride solutions that mimic hydrometallurgical process solutions. The impact of electrochemical parameters and NaCl concentration is shown to affect the efficiency of gold recovery. Further, the applied potential profile is shown to have a significant impact on both efficiency and the size distribution of the recovered gold particles on glassy carbon. Tailoring the electrochemical parameters could therefore be used to control the functional nanoparticle synthesis.

## METHODS

All solutions were prepared in deionized water (DI, 15 M $\Omega$ -cm), and the pH was adjusted with HCl (Merck, 37%) to just below 2. The chemicals used were  $\text{CuCl}_2 \cdot 2\text{H}_2\text{O}$  ( $\geq 99\%$ , Alfa Aesar), NaCl ( $\geq 99\%$ , Thermo Scientific), and gold standard for AAS ( $999 \pm 4$  mg/L, Sigma-Aldrich). All solutions in this work contained 20 g/L Cu and 5 ppm Au, unless otherwise

specified. NaCl concentrations of 0.5, 2, and 4.5 M were studied. All potentials in this work are reported against the Ag/AgCl reference electrode, unless otherwise stated. All experiments were carried out at room temperature. A WatchGas UNIMP100 was used to detect possible  $\text{Cl}_2$  evolution.

**Electrochemical Setups.** Two setups were used in this work: a typical 50 mL three-electrode cell and an electrochemical quartz crystal microbalance (EQCM) cell ( $\sim 100$   $\mu\text{L}$ ). The 50 mL cell was used for cyclic voltammetry (CV) and for the deposition of particles for particle size determination. The electrodes used in the 50 mL cell were a platinum sheet as the counter electrode (Kultakeskus Oy), a saturated calomel electrode (SCE, SI Analytics) as the reference electrode, and a glassy carbon sheet (Alfa Aesar, 1  $\text{cm}^2$ ) as the working electrode. Ivium CompactStat was used to control the experiments. A magnetic stirrer (IKA C-MAG HS 7) was used to increase mass transport in experiments studying the deposition of particles.

The glassy carbon electrodes were polished at 500 rpm (Struers LaboPol-5) on a polishing cloth (Struers, MD Mol) using water as a lubricant and 0.3  $\mu\text{m}$  alumina. Polished electrodes were rinsed with acetone, sonicated in ethanol (Etax A,  $\geq 94\%$  ethanol), rinsed with DI water, and stored in ethanol. Immediately after deposition, the electrodes were rinsed with DI water and dried with air.

A schematic of the EQCM (Biolin Scientific) cell is shown in the supporting information (Figure S1a). Sensors (Biolin Scientific, 0.97  $\text{cm}^2$  area, 5 MHz) with Au/Ti as the working electrode material were used. Other electrodes in the cell were a Ag/AgCl reference electrode (World Precision Instruments) and a Pt counter electrode (Biolin Scientific). The flow of the solution was set to 200  $\mu\text{L}/\text{min}$  using a peristaltic pump (Ismatec IPC).

**Electrochemically Assisted Reduction (EAR) Parameters.** EAR is an electrochemical pulsed reduction method. In this study, the potential applied during a pulse is termed  $E_1$  and the duration of this pulse is termed  $t_1$ . After the potential pulse, the system was allowed to be at open-circuit condition: a new pulse begins when a certain time has passed ( $t_2$ ), or the measured potential reaches a certain value ( $E_2$ ). Pulsing was repeated in each experiment  $n$  times. The impact of pulsing parameters was investigated by varying  $t_1$  between 0.01 and 10 s and  $E_1$  between 0 and 0.3 V vs Ag/AgCl, while  $E_2$  was typically 0.6 V in the EQCM cell and 0.55 V vs Ag/AgCl in the 50 mL cell used for particle characterization. A schematic representation of these parameters is shown in the Supporting Information (Figure S1b).

**Electrochemical Characterization.** Initial CV experiments were carried out to determine the relevant redox potentials. Copper (20 g/L) and gold (20 ppm) solutions were studied separately at three NaCl concentrations (0.5, 2, and 4.5 M). The potential ranges were  $-0.4$  to 1 V for copper and 0 to 1.2 V vs SCE for gold, with a 20 mV/s scan rate. All reported current density values are based on the geometric area of the electrode.

The electrochemical surface areas (ECSAs) of particles deposited on glassy carbon were measured through cyclic voltammetry in 0.1 M  $\text{H}_2\text{SO}_4$  (VWR). The upper and lower potential limits were 1.5 and 0.4 V vs Ag/AgCl, respectively, and the scan rate was 50 mV/s. The ECSA was determined from the area of the cathodic peak between 1.1 and 0.8 V. The measured charge was compared to the theoretical charge density for an oxide monolayer, which varies around 400  $\mu\text{C}$

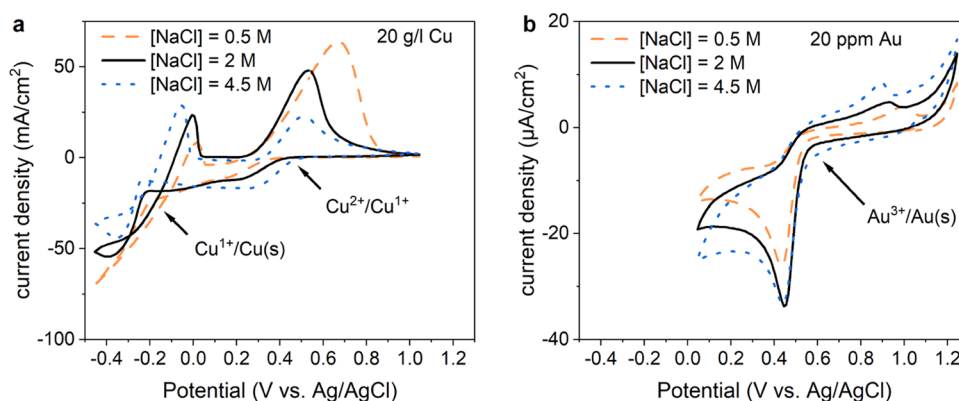


**Figure 1.** CV measurements showing the potential region of relevant reduction reactions for different NaCl concentrations. (a) Copper (20 g/L) and (b) gold (20 ppm). Scan rate 20 mV s<sup>-1</sup>.

cm<sup>-2</sup> in different studies based on crystal orientation.<sup>35</sup> Earlier studies show that 390 ± 10 µC cm<sup>-2</sup> is a good fit for polycrystalline Au,<sup>36</sup> and therefore 400 µC cm<sup>-2</sup> was used in this work. The total deposition time in the ECSA measurements was 100 s, divided into 1000 cycles of *t*<sub>1</sub> = 0.1 s for the EAR samples to obtain a signal large enough for reliable measurement.

**EQCM Data Analysis.** The process was studied in situ by EQCM. The measured frequency changes were converted to mass change using the Sauerbrey equation

$$\Delta m = -C \frac{\Delta f}{n_h} \quad (5)$$

where *m* is the electrode mass, *f* is the measured frequency, *n<sub>h</sub>* is the resonance harmonic, and *C* is the mass sensitivity constant (17.7 ng/(cm<sup>2</sup>·Hz) for the 5 MHz electrodes). The average frequency change of the most stable harmonics (3, 5, 7, and 9) was used to calculate the mass change. Current efficiency was determined by comparing the ratio of measured mass change to the theoretical value predicted by Faraday's law if only deposition of gold took place

$$\text{current efficiency} = \frac{\Delta m \cdot \nu \cdot F}{Q \cdot M_{\text{Au}}} \quad (6)$$

where *ν* is the number of electrons transferred in the reaction (1 or 3), *F* is the Faraday constant, *Q* is the total measured charge, and *M<sub>Au</sub>* is the molar mass of gold.

**Particle Size Analysis.** The deposits on glassy carbon were characterized using a scanning electron microscope (SEM, Tescan Mira3, 10 or 15 keV accelerating voltage) with integrated energy-dispersive X-ray spectroscopy (EDS, Thermo Fisher UltraDry). All samples used for surface morphology characterization were prepared using a solution with 2 M NaCl.

Particle size distributions were determined from SEM images (*N* > 5) using ImageJ, assuming spherical particles. No image processing was done to separate agglomerated particles, and therefore groups of multiple particles appear in the data as larger particles if there is no empty space between them.

## RESULTS AND DISCUSSION

**Defining EAR Parameters.** Cyclic voltammetry was performed to determine the potentials at which the key redox reactions took place (Figure 1). Copper and gold

chloride solutions were studied separately to determine the effect of chloride concentration on both.

In such high chloride concentration solutions, the predominant Cu<sup>2+</sup> complex is suggested to be CuCl<sub>4</sub><sup>2-</sup>, whereas the most stable Cu<sup>1+</sup> complexes are CuCl<sub>2</sub><sup>-</sup> and CuCl<sub>3</sub><sup>2-</sup>.<sup>37,38</sup> For the copper solution (Figure 1a), two onset potentials for reduction can be seen. These correspond to Cu<sup>2+</sup>/Cu<sup>1+</sup> around 0.4 V and Cu<sup>1+</sup>/Cu around -0.2 V vs Ag/AgCl. As the chloride concentration increases, the potential region between Cu<sup>2+</sup> to Cu<sup>1+</sup> reduction and Cu<sup>1+</sup> to Cu reduction widens. This is attributed to the stabilizing effect of chlorides on cuprous species.<sup>34,37</sup>

Gold solutions were prepared with gold in the trivalent state Au<sup>3+</sup>. The dominant Au<sup>3+</sup> chloride complex at low pH is AuCl<sub>4</sub><sup>-</sup>,<sup>39</sup> while for Au<sup>1+</sup>, it is AuCl<sub>2</sub><sup>-</sup>.<sup>7</sup> Cyclic voltammetry (Figure 1b) suggests that the NaCl concentration has much less impact on gold species redox potentials in comparison with copper solutions. The cathodic scan showed only one clear reduction peak at approximately 0.55 V vs Ag/AgCl, which was attributed to the reduction of aqueous to solid Au, and its onset potential increased only slightly with increasing NaCl concentration. During the reverse scan, a slight increase in the anodic current was seen at >0.6 V, which peaked around 0.8–1 V vs Ag/AgCl. This peak was attributed to the oxidation of gold back into the solution, and the low anodic current compared to the reduction peak means that this oxidation appeared to be inhibited, as has been reported in other studies.<sup>40</sup> A second anodic peak can be seen at >1.1 V vs Ag/AgCl, which may be related to Au<sup>1+</sup>/Au<sup>3+</sup>, overlapping with oxygen evolution based on the bubbles appearing on the electrode. However, the anodic behavior of gold in various chloride concentrations has been explored extensively elsewhere<sup>31,41,42</sup> and was not studied further here. For this work, the most relevant information obtained from the CV measurements is that aqueous gold is reduced to elemental gold at potentials more negative than 0.55 V vs Ag/AgCl, showing that gold species remain slightly more noble than cupric species in all of the NaCl concentrations studied, thus supporting the use of the EAR method.

The aim of this work is to study the Cu<sup>1+</sup>-mediated path for gold recovery as nanoparticles. Therefore, based on the CV measurements presented in Figure 1, 0–0.3 V was chosen as the potential (*E*<sub>1</sub>) region of interest since in this potential region, Cu<sup>2+</sup>/Cu<sup>1+</sup> reduction can occur for all studied NaCl concentrations, which is a requirement for EAR. The driving force of gold reduction onto the electrode in this case (eqs 2

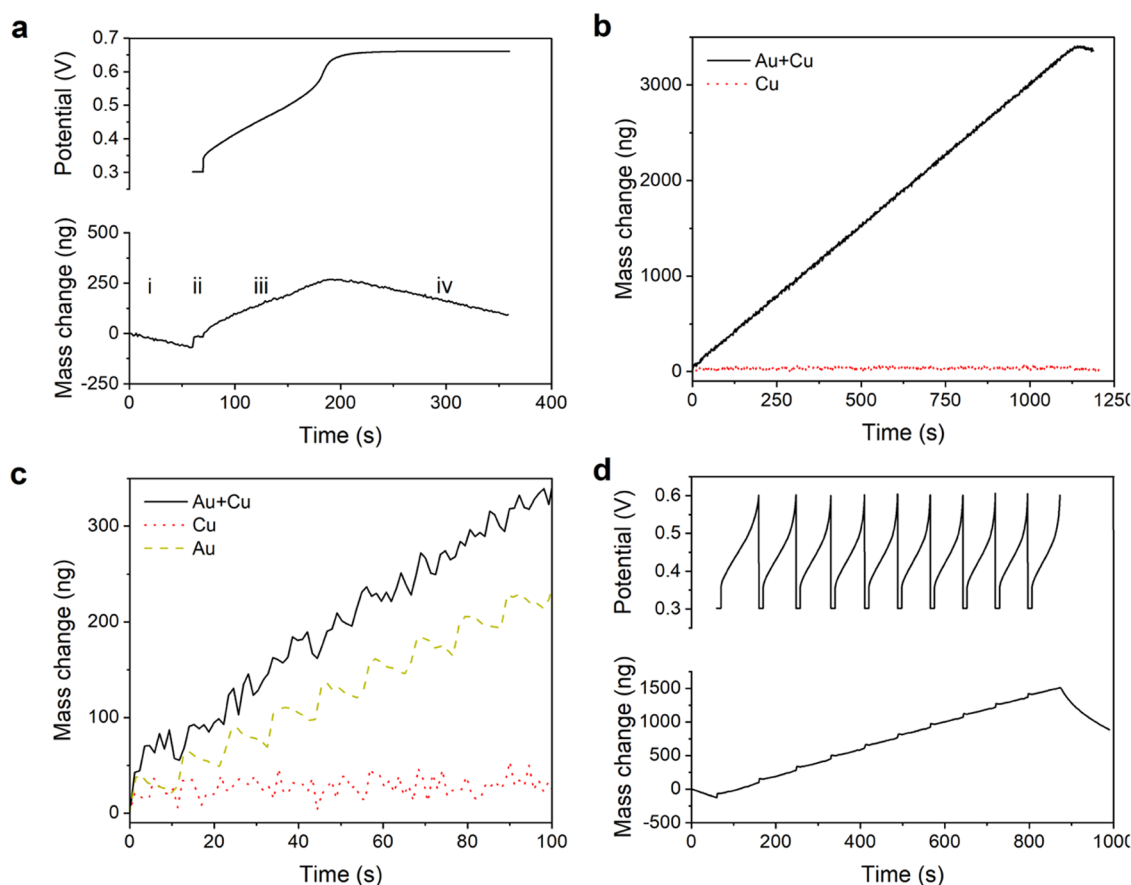


**Figure 2.** (a) Single EAR deposition cycle divided into four phases: dissolution (i), potential pulse for Cu<sup>2+</sup> reduction to Cu<sup>1+</sup> (ii), reduction of Au species by Cu<sup>1+</sup> and deposition of Au (iii), and redissolution (iv). (b) 100 cycles of EAR with and without gold. (c) The first 100 s of mass change for gold- and copper-containing solutions during potential pulsing. (d) Ten cycles of EAR with an E<sub>2</sub> limit of 0.6 V vs Ag/AgCl results in an almost linear mass increase. For all measurements, flow rate = 200 μL/min, E<sub>1</sub> = 0.3 V. For (a) and (d) t<sub>1</sub> = 10 s. For (b) and (c), t<sub>1</sub> = 1 s and t<sub>2</sub> = 10 s. Solutions contained 5 ppm Au, 20 g/L Cu, and 2 M NaCl.

and 4) is the nobility difference between dissolved gold and cuprous chloride complexes. Lowering the NaCl concentration increases this driving force since it has a greater impact on the reduction potential of Cu<sup>2+</sup>/Cu<sup>1+</sup> than that of Au<sup>3+</sup>/Au.

**Gold Recovery through EAR.** Three features impeded the electrochemical reduction of gold from the cupric chloride solutions studied in this work: the large concentration difference between Au and Cu, the nearly overlapping reduction potentials with copper, and the solution's corrosive nature toward gold. It has been demonstrated that cupric chloride will effectively corrode gold and that the corrosion potential is approximately 0.6 V vs SCE (~0.65 V vs Ag/AgCl) for various cupric ion concentrations.<sup>7,43</sup> In addition, AuCl<sub>4</sub><sup>-</sup> has been shown to corrode metallic gold in the presence of complexing ions.<sup>44,45</sup> EQCM measurements were carried out in order to better understand the relationship between gold reduction and corrosion within these solutions.

EQCM measurements of pulsed potential showed that material is deposited on the electrode both during and between electrochemical potential pulses. Figure 2a shows how the electrode's mass changes during one pulse (t<sub>1</sub> = 10 s, E<sub>1</sub> = 0.3 V) can be divided into four phases. Before deposition (Phase i), the mass of the gold electrode is reduced by corrosion. During the potential pulse (t<sub>1</sub>, Phase ii), the electrode's mass increases sharply due to the direct deposition of gold. Then, after the potential pulse, the electrode's mass increases gradually (t<sub>2</sub>, Phase iii) until it reaches a maximum and then

is again decreased due to corrosion (Phase iv). Apart from Phase ii, the cell is in the open-circuit condition where no current passes through the cell, and so the buildup of mass during Phase iii is attributed to the spontaneous reduction of gold by cuprous species generated by the potential pulse. Notably, this experiment shows that the EAR process can indeed be used for gold recovery onto electrodes from cupric chloride solutions at lower overpotentials than those which have been shown for EDRR, as speculated by Korolev et al.<sup>27</sup> The energy requirement of an electrochemical reaction is directly related to the applied potential, and so developing recovery methods that require less applied potential is central to the green chemistry principle of *Design for Energy Efficiency*.<sup>46</sup>

Gold was chosen as the working electrode material to avoid contamination from other elements. However, it is important to consider the contribution of dissolved gold to the measured mass increase, and we found it to be minimal. Based on earlier studies, gold is dissolved by cupric chloride as Au<sup>1+</sup> but can then further react to form Au<sup>3+</sup> and metallic Au through disproportionation.<sup>7</sup>

As a result of these corrosion processes, there may be both Au<sup>1+</sup> and Au<sup>3+</sup> species in the solution when deposition begins. Therefore, longer measurements were conducted to determine the contribution of the gold in the initial solution and the gold dissolved from the electrode to the measured mass increase during Phase ii. Pulsed EAR was carried out for 100 cycles

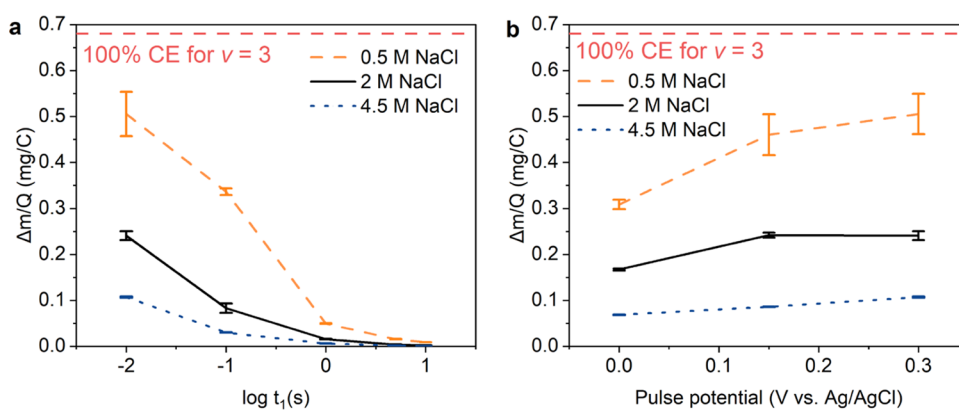


**Figure 3.** Measured mass increase per charge for gold recovery as a function of (a) pulse time and (b) pulse potential. For (a), the pulse potential was kept at 0.3 V vs Ag/AgCl, and for (b), the pulse duration was kept at 0.01 s. The dashed red line represents 100% current efficiency for a three-electron process (valence of Au  $\nu = 3$ , eq 6). Pulse duration was determined by an OCP limit of 0.6 V. Error bars represent standard error.

from copper chloride solutions with and without the addition of gold (Figure 2b). Potential pulsing in the absence of gold did not result in any mass buildup on the electrode, whereas a significant mass increase was seen when gold was present in the solution. Also, any gold dissolved from the electrode before the measurement was likely to be spent or to have flowed out of the cell during the first few cycles, but the recovery rate remained nearly constant throughout the measurement. This confirms that it is indeed the gold in the solution, rather than the gold dissolved from the electrode, that is responsible for most of the mass increase, i.e., gold recovery. It also shows that not only  $\text{Au}^{1+}$  but also  $\text{Au}^{3+}$  solutions are suitable for recovery through spontaneous reduction by  $\text{Cu}^{1+}$ , such as the EAR method presented here. Since  $\text{Au}^{3+}$  is present as  $\text{AuCl}_4^-$ , we posit that the mass increase between potential pulses proceeds mostly according to eq 4. However, it is still unclear whether  $\text{Au}^{3+}$  is reduced to metallic gold directly or if it is first reduced to  $\text{Au}^{1+}$  and then further to metallic gold according to eq 2.

To further investigate the role of copper in the EAR process, pulsed deposition at 0.3 V was carried out in solutions containing no copper, but only 5 ppm  $\text{Au}^{3+}$  and 2 M NaCl (Figure 2c). These solutions were also corrosive toward the gold electrode, which shows that  $\text{Au}^{3+}$  also significantly contributes to the corrosion in our system. In these solutions, the deposition proceeds rapidly during the potential pulse and corrodes between them. Under the same pulsing conditions in the solution containing only copper and no gold, the mass of the electrode remained relatively constant. This was attributed to the  $\text{Cu}^{1+}$  species generated by the potential pulse between the electrode and the corrosive bulk solution. When the solution contained both gold and copper, the mass of the electrode increases steadily, without distinct periods of deposition and corrosion.

The spontaneous buildup of mass on the electrode during Phase iii (Figure 2a) coincided with increasing OCP (open-circuit potential), which reflects the changing conditions at the electrode/solution interface caused both by the reduction of gold onto the electrode and the flow of the solution. As can be seen from Figure 2a, OCP reaches equilibrium at the same time as the electrode starts to corrode. Based on these findings, the cuprous species act as a barrier that prevents the corrosion of the electrode by cupric species. Therefore, limiting the OCP between each pulse is an efficient way to maximize the gold recovery of each cycle without risking corrosion. By setting an OCP limit ( $E_2$ ) at 0.6 V vs Ag/AgCl as the starting condition

for a new pulse, a steady buildup of gold on the electrode can be achieved (Figure 2d) by applying a pulsed potential profile.

An important difference can be observed between the EAR measurements of Figure 2 and the EDRR measurements reported by Korolev et al.<sup>27</sup> Each EDRR cycle includes the deposition of metallic copper followed by its oxidation by cupric species according to eq 1. From the gold recovery point of view, all of the deposited copper that does not react with gold can lower the current efficiency. In the EAR process, on the other hand, current efficiency is determined by the ratio of the generated cuprous species that react with gold. Therefore, the dependence of this ratio on the process parameters was studied further.

The impact of NaCl concentration, pulse time ( $t_1$ ), and pulse potential ( $E_1$ ) on current efficiency is shown in Figure 3. Since the exact ratio of  $\text{Au}^{3+}$  to  $\text{Au}^{1+}$  was unknown, mass change per charge was used as the figure of merit, where 0.68 mg/C corresponds to 100% current efficiency for a three-electron process. The real current efficiencies are likely closer to Au valence  $\nu = 3$  (eq 6), since gold is added as a trivalent when making the solution, and due to the flow of the solution, the corrosion products should not accumulate in the cell. The average measured mass change, charge, and current efficiencies (CE) calculated according to eq 6 can be found in Supporting Information Tables S1–S3: the calculations are done for varying NaCl concentrations, i.e., 0.5 M (Table S1), 2 M (Table S2), and 4.5 M (Table S3). Even if we assume that the most likely scenario in this study is  $\nu = 3$ , the current efficiency values are presented for both valence states,  $\nu = 1$  or 3.

A clear trend could be observed: decreasing  $t_1$  increased current efficiency. For the 2 M NaCl solution, the change was from approximately 0.002 mg/C (CE 0.3% for  $\nu = 3$ ) for  $t_1 = 10$  s to 0.24 mg/C (CE 35% for  $\nu = 3$ ) for  $t_1 = 0.01$  s. Changing  $E_1$  had a similar effect, as minimal overpotential resulted in the best current efficiency. For the 2 M NaCl solution, the current efficiency changed from 0.24 mg/C at 0.3 V to 0.17 mg/C (CE 25% for  $\nu = 3$ ) at 0 V vs Ag/AgCl. Finally, increasing the concentration of NaCl in the solution significantly lowered the current efficiency for all deposition parameters, with the best efficiency of  $\sim 0.5$  mg/C (CE 74% for  $\nu = 3$ ) measured for the 0.5 M NaCl solution at  $t_1 = 0.01$  s and  $E_1 = 0.3$  V vs Ag/AgCl.

All of the results point to better current efficiency when the reactions are kept minimal, i.e., minimizing the cuprous chloride generation per cycle. For the reduction of gold onto

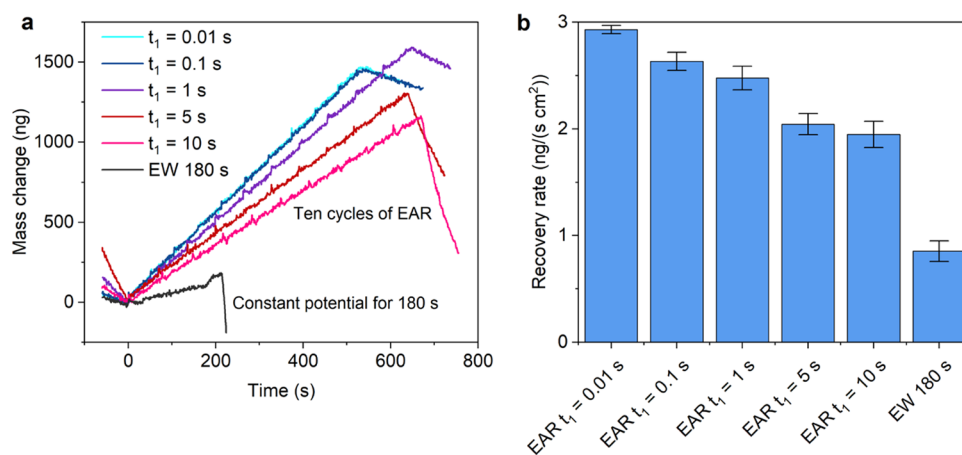


**Figure 4.** Increasing the pulse duration lowered the rate of recovery and increased the rate of dissolution once polarization ended. (a) Mass change and (b) rate of recovery as a function of time for EAR using various  $t_1$ . For (b), the average rate and standard error are calculated from  $N \geq 3$  measurements.  $E_1$  was 0.3 V vs Ag/AgCl, and all measurements consisted of 10 cycles of deposition, except for EW 180 s, for which the potential was kept at 0.3 V (electrowinning). [NaCl] = 2 M.

the electrode, it is sufficient to maintain a region of cuprous species near the electrode. A longer pulse or increased overpotential seems to increase the portion of cuprous species that migrate away from the electrode and therefore never contribute to the measured gold recovery. Similarly, since increasing the chloride concentration promotes the  $\text{Cu}^{2+} \rightarrow \text{Cu}^{1+}$  reduction reaction (Figure 1a), the same potential pulse will generate more cuprous species in higher chloride concentration solutions. Furthermore, the nobility difference between aqueous cuprous and gold chloride species is also greatest at low salt concentrations. Nevertheless, spontaneous deposition with over 10% current efficiency ( $\nu = 3$ ) was shown to occur between pulses even at 4.5 M NaCl concentration.

Current efficiencies for electrochemical metal recovery from dilute solutions reported in the literature vary significantly due to the variation in the solutions and processes studied. For gold recovery via electrowinning, Kasper et al.<sup>47</sup> reported a ~3% current efficiency from ammoniacal thiosulfate, and Brandon et al.<sup>48</sup> and Barbosa et al.<sup>49</sup> reported less than 1% current efficiency for dilute cyanide solutions. In this work, the current efficiency of electrowinning was even lower (<0.1%, Table S2) since the copper reduction reaction dominated at all studied potentials due to the large concentration difference between gold and copper. Thus, electrowinning is only suitable for the narrow potential region where there are no competing reactions, and this limits its ability to be used for fabricating functional surfaces from complex solutions. Pretreatment, i.e., purification of leaching solutions, is usually a necessity for industrial EW processes to obtain high-purity products.<sup>50–52</sup> In contrast, EAR can use suitable impurities such as copper to achieve greater current efficiency while operating in the potential region where competing reactions occur.

It was also observed that the recovery rate of gold decreased when  $t_1$  increased, which indicates that the  $\text{Cu}^{2+}/\text{Cu}^{1+}$  reaction hinders gold deposition (Figure 4). If this were not the case, the highest recovery rate would be expected for electrowinning, where the constantly applied potential reduces all gold flowing past to the electrode. As with current efficiency, a likely explanation is that longer pulses generate more excess cuprous species, which then migrate away from the electrode. These may then react with gold in the bulk solution or near another surface, thus hindering the flow of gold to the

electrode. To support this argument, the current efficiency and rate of recovery were also measured with a solution containing four times more gold (20 ppm Au, 2 M NaCl, 20 g/L Cu). In this experiment, more gold can be transported to the electrode before the cuprous species have transferred away, and so both current efficiency and rate of recovery are expected to increase. Indeed, compared to the solution with 5 ppm Au, the recovery efficiency increased from 0.1 to 0.18 mg/C for  $t_1 = 0.1$  and from 0.24 to 0.43 mg/C for  $t_1 = 0.01$  s. Likewise, the rate of recovery increased to ~10.8 ng/s for  $t_1 = 0.1$  and to ~11.2 ng/s for  $t_1 = 0.01$  s. The measured mass change profiles can be found in the Supporting Information (Figure S2).

In addition, longer pulse times lead to more rapid dissolution once polarization ended (Figure 4a). Since small changes in pH should not affect the dissolution rate,<sup>31</sup> the cause is likely the generation of corrosive species on the anode. Indeed, the OCP increased sharply during the corrosion (Figure S3), indicating the presence of a strong oxidant such as aqueous chlorine, which could negatively affect the process efficiency by oxidizing the generated cuprous species.<sup>53</sup> As such, low pulse times were found optimal for process efficiency, rate of recovery, and stability.

All of the EQCM measurements were run with solution flow (200  $\mu\text{L}/\text{min}$ ) through the cell. Many commercial electro-winning processes also operate with flow.<sup>54</sup> In our case, the mass transport of gold and copper species from the electrode is therefore influenced both by flow and diffusion. Without flow, the recovery of gold by EAR was found to proceed significantly slower (Supporting Information Figure S4). Barbosa et al.<sup>49</sup> also found that controlling the flow rate could enhance the effectiveness of gold extraction from diluted cyanide solutions. Agitation of the solution to enhance mass transport is therefore important when considering scale-up of the process since it can minimize the dwell time of the solution, which still contains many valuable elements that can in turn can be recovered downstream.

An important consideration is also the underpotential deposition (UPD) of copper on the Au electrode. The galvanic replacement of such a deposited monolayer could also explain a gradual increase of the measured mass. However, in our case, cyclic voltammetry on the Au/Ti electrodes (Figure S5) showed no evidence of UPD, which would typically result

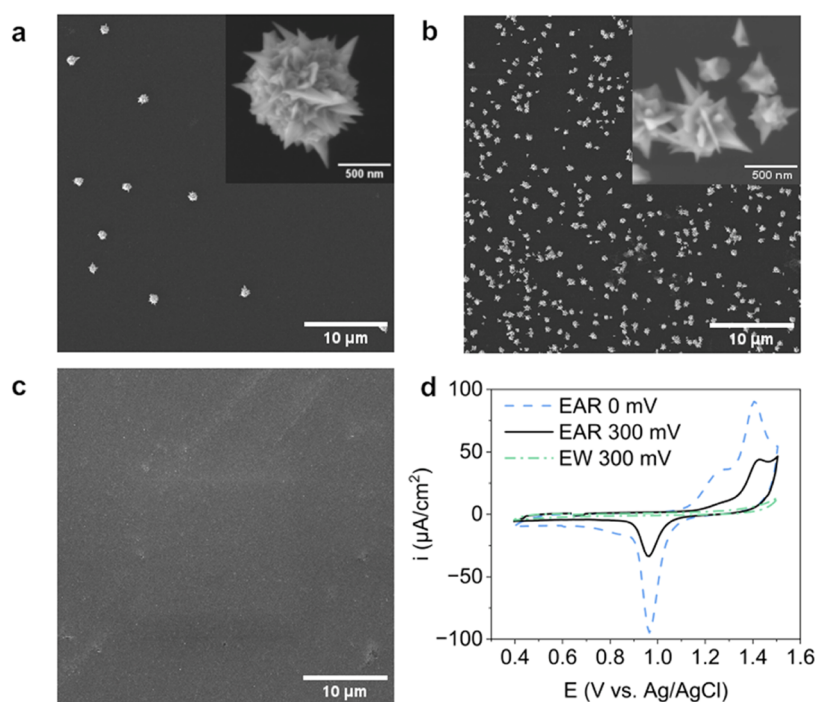


**Figure 5.** (a–c) SEM images of the impact of pulse time and potential on gold deposition onto glassy carbon. (a) EAR at 300 mV,  $t_1 = 0.1$  s, 1000 cycles; (b) 0 mV,  $t_1 = 0.1$  s, 1000 cycles; (c) electrowinning at 300 mV for 100 s. Deposition solution: 5 ppm Au, 20 g/L Cu, and 2 M NaCl. (d) CV measurements in 0.1 M H<sub>2</sub>SO<sub>4</sub> of samples (a–c) showing gold oxidation and reduction peaks, scan rate 50 mV/s.

in a distinct peak on the anodic scan.<sup>55,56</sup> EDS analysis of the QCM electrodes after polarization at 300 mV also showed no copper deposition (Figure S6). Finally, the shape of the measured mass increase profile would be expected to be different for UPD: each pulse would be expected to rapidly increase the mass of the electrode. Instead, only a small mass change is seen from each potential pulse, which can also result from the direct deposition of gold. These results support the aqueous Cu<sup>1+</sup> mediated process.

**Deposition of Gold Particles and Particle Size Control.** The ability to directly create functional surfaces, rather than recovering metal for further refinement, could make the processing of low-concentration solutions more attractive. Therefore, gold was deposited onto glassy carbon electrodes by the EAR process to determine the impact of electrochemical parameters on deposit morphology. To determine the impact of  $E_1$ , 1000 cycles of EAR at  $E_1 = 300$  and 0 mV vs Ag/AgCl were compared, with  $t_1 = 0.1$  s and  $E_2 = 550$  mV (Figure 5a,b). Also, in order to compare EAR to direct electrowinning, deposition was carried out at a constant potential (Figure 5c) for the same total deposition time of 100 s. The electrochemically active surface area (ECSA) of deposited gold was measured with cyclic voltammetry in 0.1 M H<sub>2</sub>SO<sub>4</sub> since this parameter can be used for both comparing the recovery efficiency and the suitability of the resulting surface for electrochemical applications such as sensing or catalysis.

First, the results show that EAR was significantly more effective than EW at these potentials. SEM images of the electrode after 100 s of EW at 300 mV vs Ag/AgCl showed practically no gold deposition, whereas after EAR at the same potential, gold particles were observed (Figure 5a,c, EDS analysis in supporting information Figures S7–S10). Measurements of the ECSA showed almost no reductive peak for

samples prepared by EW at 300 mV (Figure 5d). The ECSA values for the different deposition approaches are shown in Table 1. These results are in line with the findings of EQCM measurements, where EAR outperformed EW for gold recovery.

**Table 1. Electrochemical Surface Area after EAR and EW Deposition at Different Potentials<sup>a</sup>**

deposition method	$E_1$ (mV vs Ag/AgCl)	nucleation pulse	ECSA (cm <sup>2</sup> /cm <sup>2</sup> )
EAR	300		0.18
EAR	0		0.42
EW	300		$7.3 \times 10^{-4}$
EW	0		$7.0 \times 10^{-3}$
EAR	300	−500 mV	0.53

<sup>a</sup>Total deposition time of 100 s for all samples, divided into 1000 cycles of  $t_1 = 0.1$  s for EAR. The ECSA value is the average of three measurements.

Second, increasing the overpotential resulted in more deposition. EAR with  $E_1 = 0$  mV resulted in significantly higher particle coverage than with 300 mV. The measured ECSA was also over two times larger (0.42 vs 0.18 cm<sup>2</sup>/cm<sup>2</sup>). For comparison, deposition was also carried out by EW at 0 mV for 100 s. Again, EW deposition was less effective than EAR. However, some particles were seen covering the electrode surface (Supporting Information Figure S11), although they were too small for EDS analysis. Nevertheless, the ECSA measurement showed a small reductive peak, indicating that these features were gold particles. This signal was an order of magnitude greater than for EAR at 300 mV (Table 1). As such, deposition at a larger overpotential was more effective for both EAR and EW approaches.

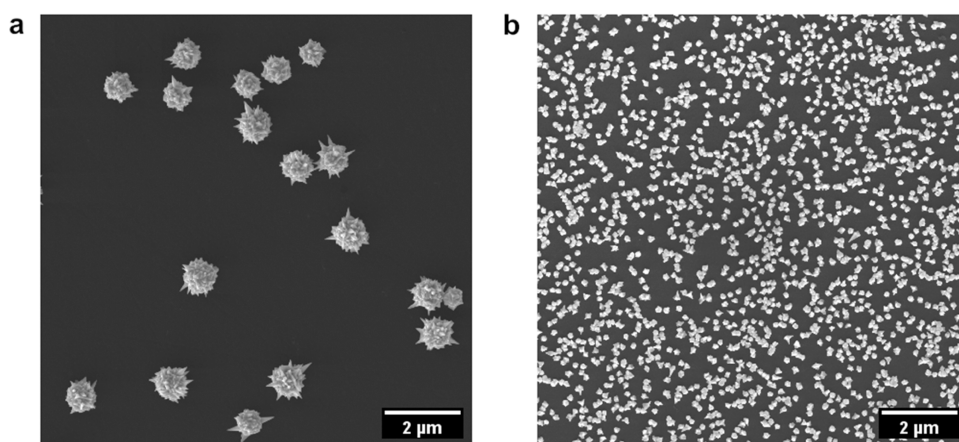


**Figure 6.** Addition of a 0.1 s nucleation pulse at  $-500$  mV before deposition has a large impact on gold recovery with EAR on glassy carbon. SEM images of samples prepared (a) without and (b) with a nucleation pulse. Other deposition parameters:  $E_1 = 300$  mV,  $t_1 = 0.1$  s,  $E_2 < 550$  mV vs Ag/AgCl.

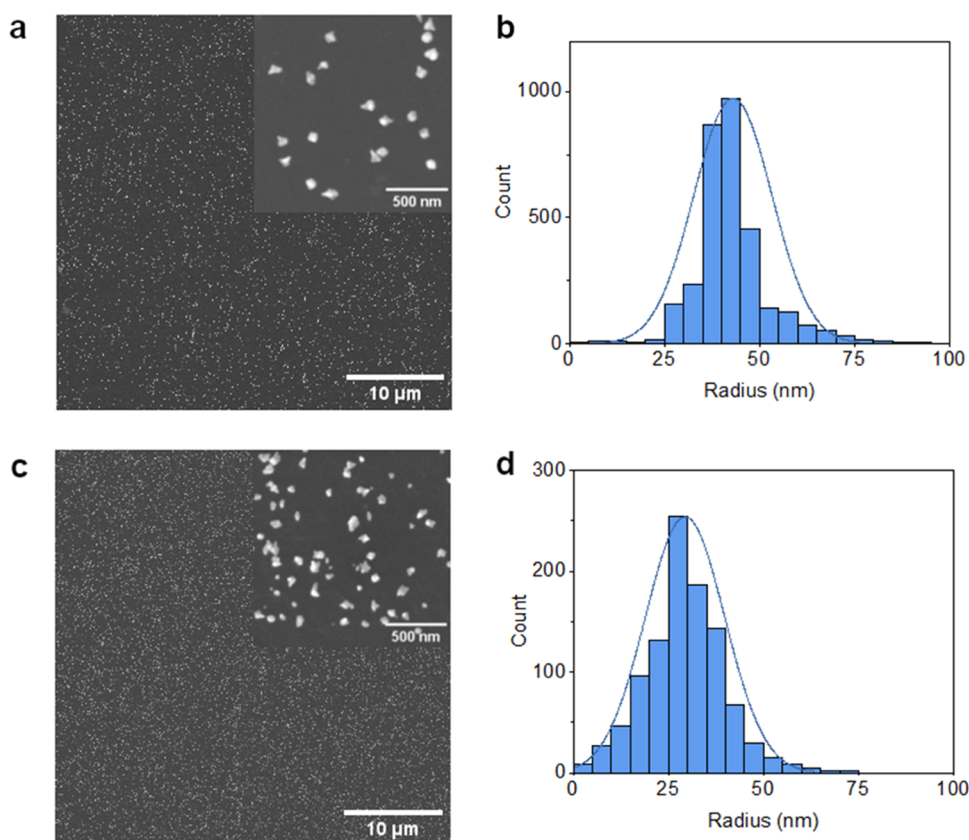


**Figure 7.** SEM images and particle size distributions of samples prepared with (a, b) a nucleation pulse at  $-500$  mV for 0.1 s,  $E_1 = 300$  mV, and (c, d) no nucleation pulse,  $E_1 = 0$  mV. For both samples,  $t_1 = 0.1$  s,  $E_2 = 550$  mV vs Ag/AgCl, and cycles = 100.

While in the EQCM measurements greatest current efficiency was achieved with the lowest overpotential (Tables S1–S3), on glassy carbon, using higher overpotential resulted in higher particle coverage. A likely explanation for this difference is the electrode material, which was gold for EQCM. It has been shown that nucleation depends on the overpotential and the substrate material.<sup>57</sup> If gold recovery through EAR (eqs 2 and 4) occurs preferentially on gold, then the reaction on glassy carbon may be limited by the amount of suitable nucleation sites.

Indeed, the particle size distribution of EAR at 0 mV vs Ag/AgCl is clearly broad (Figure 5b). This is typical behavior in the pulsed electrodeposition of particles, as each cycle results in both new nucleation and the growth of previously deposited particles.<sup>24</sup> By contrast, the particle size of EAR at 300 mV vs Ag/AgCl appears more uniform and the coverage is less dense (Figure 5a), indicating that nucleation may have been the limiting factor. It was also found that the particle density was reduced when going from 100 to 1000 cycles, which indicates that Ostwald ripening occurs during the process (Supporting Information Figure S12).

Based on these findings, a nucleation pulse of high overpotential may improve the efficiency of EAR on glassy carbon by populating the surface with sites for growth. To test this, samples were prepared with the addition of a single 0.1 s potential pulse at  $-500$  mV followed by EAR at  $300$  mV for  $1000$  cycles (same parameters as in Figure 5a). The addition of this single nucleation potential pulse was shown to have a significant impact on the recovery (Figure 6). This effect is also reflected in the measured electrochemical surface area (Table 1) which was more than doubled by the inclusion of a nucleation pulse ( $0.18$  to  $0.53$   $\text{cm}^2/\text{cm}^2$ ). As the difference in these samples only occurred in the first  $0.1$  s, we can determine that the role of the surface material is significant for EAR. Also, as the pulse potential of  $300$  mV is more positive than the oxidation potential of metallic copper (Figure 1a), any copper that may be deposited during the nucleation pulse will be oxidized back into the solution as  $\text{Cu}^{1+}$  instead of remaining as an impurity on the surface.

Since effective nucleation on glassy carbon appears to require a high overpotential, the approach of starting with a nucleation pulse followed by low overpotential EAR could in effect separate the nucleation and growth of the particles. This is a classic approach for the preparation of uniform-sized nanoparticles and demonstrated for electrodeposition by Penner et al.<sup>24</sup> Here, samples were prepared with  $100$  cycles of growth to measure the particle size distribution. Two approaches were compared: the first being a nucleation pulse at  $-500$  mV for  $0.1$  s followed by EAR at  $300$  mV (Figure 7a,b) and the second being no nucleation pulse and  $E_1 = 0$  mV (Figure 7c,d).

The particle size distribution was noticeably different between the approaches of a nucleation pulse with low overpotential growth ( $43 \pm 10$  nm) and using a high overpotential each cycle ( $29 \pm 10$  nm). Smaller particles (radius  $< 25$  nm) especially were less common on the samples prepared with a nucleation pulse, indicating that the separation of nucleation and growth was at least partially successful. Importantly, these results demonstrate that the particle size and size distribution can be controlled in the EAR process by the applied potential.

Like EDRR, EAR was shown to be able to selectively recover gold without added chemicals from relatively low concentrations. Operating at a more positive potential than EDRR, EAR demonstrated some advantages for nanoparticle deposition: distinctive particles which can be tailored with the applied potential, and higher purity since no copper is reduced to the surface.

## CONCLUSIONS

This study demonstrated the selective deposition of gold through electrochemically assisted aqueous reduction in cupric-gold chloride solutions. This EAR process was found to be sensitive to changes in pulse time, pulse potential, and surface material. The spontaneous reduction between  $\text{Cu}^{1+}$  and aqueous gold species was observed at all studied NaCl concentrations ( $0.5$ ,  $2$ , and  $4.5$  M), but the process was the most efficient at the lowest NaCl concentration where the nobility difference and thus the driving force for gold reduction by  $\text{Cu}^{1+}$  was also greatest.

On glassy carbon, populating the substrate with gold by first applying a  $0.1$  s nucleation pulse at  $-500$  mV greatly enhanced gold recovery at  $300$  mV (ECSA after  $1000$  cycles  $0.53$   $\text{cm}^2/\text{cm}^2$  with and  $0.18$   $\text{cm}^2/\text{cm}^2$  without a nucleation pulse). By

changing the applied potential profile, the particle size distribution and shape of the recovered gold particles could be influenced.

It is likely that EAR is suitable for metal pairs other than the copper and gold studied in this work. As such, future research should also consider other metals commonly present in metallurgical solutions. Overall, understanding how the products of certain competing reactions can be harnessed for the deposition of noble metals can lead to more efficient utilization of complex metal solutions.

## ASSOCIATED CONTENT

### Data Availability Statement

Data for this paper, including electrochemical, QCM, and EDS data, as well as SEM images of deposited particles, are available at Zenodo at [10.5281/zenodo.7660056](https://doi.org/10.5281/zenodo.7660056).

### Supporting Information

The Supporting Information is available free of charge at <https://pubs.acs.org/doi/10.1021/acs.jpcc.3c03135>.

Additional experimental details, including table values of current efficiency, corrosion rate, and SEM/EDS characterization (PDF)

## AUTHOR INFORMATION

### Corresponding Author

Kirsi Yliniemi – School of Chemical Engineering, Aalto University, Espoo 02150, Finland; [orcid.org/0000-0003-2536-388X](https://orcid.org/0000-0003-2536-388X); Phone: +358505923690; Email: [kirsi.yliniemi@aalto.fi](mailto:kirsi.yliniemi@aalto.fi)

### Authors

Reima Herrala – School of Chemical Engineering, Aalto University, Espoo 02150, Finland; [orcid.org/0000-0001-5870-050X](https://orcid.org/0000-0001-5870-050X)

Zulin Wang – School of Chemical Engineering, Aalto University, Espoo 02150, Finland; [orcid.org/0000-0002-2234-7983](https://orcid.org/0000-0002-2234-7983)

Jaana Vapaavuori – School of Chemical Engineering, Aalto University, Espoo 02150, Finland; [orcid.org/0000-0002-5923-0789](https://orcid.org/0000-0002-5923-0789)

Mari Lundström – School of Chemical Engineering, Aalto University, Espoo 02150, Finland

Complete contact information is available at:

<https://pubs.acs.org/10.1021/acs.jpcc.3c03135>

### Author Contributions

R.H.: Methodology, investigation, formal analysis, visualization, writing—original draft, writing—review & editing. Z.W.: Methodology, writing—review & editing. J.V.: Supervision, conceptualization, funding acquisition, writing—review & editing. M.L.: Supervision, conceptualization, funding acquisition, writing—review & editing. K.Y.: Supervision, conceptualization, funding acquisition, writing—review & editing.

### Notes

The authors declare no competing financial interest.

## ACKNOWLEDGMENTS

This work was supported by the Academy of Finland project EARMetal (LC, KY, ML: 339979 and LC, KY, JV: 342080). The authors also acknowledge the RawMatTERS Finland

Infrastructure funded by the Academy of Finland and located at Aalto University.

## REFERENCES

- (1) European Commission. Roadmap to a Resource Efficient Europe, 2011. [https://ec.europa.eu/environment/resource\\_efficiency/about/roadmap/index\\_en.htm](https://ec.europa.eu/environment/resource_efficiency/about/roadmap/index_en.htm) (accessed June 17, 2023).
- (2) International Energy Agency. Renewables 2021 - Analysis and Forecast to 2026. <https://www.iea.org/reports/renewables> (accessed 14 October 2022).
- (3) Hyvärinen, O.; Hämäläinen, M. HydroCopper—a New Technology Producing Copper Directly from Concentrate. *Hydrometallurgy* **2005**, *77*, 61–65.
- (4) McDonald, R. G.; Whittington, B. I. Atmospheric Acid Leaching of Nickel Laterites Review. Part II. Chloride and Bio-Technologies. *Hydrometallurgy* **2008**, *91*, 56–69.
- (5) Altinkaya, P.; Liipo, J.; Kolehmainen, E.; Haapalainen, M.; Leikola, M.; Lundström, M. Leaching of Trace Amounts of Metals from Flotation Tailings in Cupric Chloride Solutions. *Min. Metall. Explor.* **2019**, *36*, 335–342.
- (6) Rinne, M.; Elomaa, H.; Seisko, S.; Lundström, M. Direct Cupric Chloride Leaching of Gold from Refractory Sulfide Ore: Process Simulation and Life Cycle Assessment. *Miner. Process. Extr. Metall. Rev.* **2022**, *43*, 598–609.
- (7) Lampinen, M.; Seisko, S.; Forsström, O.; Laari, A.; Aroma, J.; Lundström, M.; Koironen, T. Mechanism and Kinetics of Gold Leaching by Cupric Chloride. *Hydrometallurgy* **2017**, *169*, 103–111.
- (8) Kesler, S. E.; Chryssoulis, S. L.; Simon, G. Gold in Porphyry Copper Deposits: Its Abundance and Fate. *Ore Geol. Rev.* **2002**, *21*, 103–124.
- (9) Toro, N.; Moraga, C.; Torres, D.; Saldaña, M.; Pérez, K.; Gálvez, E. Leaching Chalcocite in Chloride Media—A Review. *Minerals* **2021**, *11*, 1197.
- (10) Liddicoat, J.; Dreisinger, D. Chloride Leaching of Chalcopyrite. *Hydrometallurgy* **2007**, *89*, 323–331.
- (11) Sheridan, E.; Hjelm, J.; Forster, R. J. Electrodeposition of Gold Nanoparticles on Fluorine-Doped Tin Oxide: Control of Particle Density and Size Distribution. *J. Electroanal. Chem.* **2007**, *608*, 1–7.
- (12) Vahdatkhab, P.; Sadrezhaad, S. K. Influence of Substrate, Additives, and Pulse Parameters on Electrodeposition of Gold Nanoparticles from Potassium Dicyanoaurate. *Metall. Mater. Trans. B* **2015**, *46*, 2584–2592.
- (13) Monteiro, M. C. O.; Philips, M. F.; Schouten, K. J. P.; Koper, M. T. M. Efficiency and Selectivity of CO<sub>2</sub> Reduction to CO on Gold Gas Diffusion Electrodes in Acidic Media. *Nat. Commun.* **2021**, *12*, No. 4943.
- (14) Lu, Q.; Rosen, J.; Zhou, Y.; Hutchings, G. S.; Kimmel, Y. C.; Chen, J. G.; Jiao, F. A Selective and Efficient Electrocatalyst for Carbon Dioxide Reduction. *Nat. Commun.* **2014**, *5*, No. 3242.
- (15) Hvolbæk, B.; Janssens, T. V. W.; Clausen, B. S.; Falsig, H.; Christensen, C. H.; Nørskov, J. K. Catalytic Activity of Au Nanoparticles. *Nano Today* **2007**, *2*, 14–18.
- (16) Yogi, C.; Kojima, K.; Hashishin, T.; Wada, N.; Inada, Y.; Della Gaspera, E.; Bersani, M.; Martucci, A.; Liu, L.; Sham, T.-K. Size Effect of Au Nanoparticles on TiO<sub>2</sub> Crystalline Phase of Nanocomposite Thin Films and Their Photocatalytic Properties. *J. Phys. Chem. C* **2011**, *115*, 6554–6560.
- (17) Moitra, P.; Alafeef, M.; Dighe, K.; Frieman, M. B.; Pan, D. Selective Naked-Eye Detection of SARS-CoV-2 Mediated by N Gene Targeted Antisense Oligonucleotide Capped Plasmonic Nanoparticles. *ACS Nano* **2020**, *14*, 7617–7627.
- (18) Chiang, H.-C.; Wang, Y.; Zhang, Q.; Levon, K. Optimization of the Electrodeposition of Gold Nanoparticles for the Application of Highly Sensitive, Label-Free Biosensor. *Biosensors* **2019**, *9*, 50.
- (19) Chai, C.; Gao, J.; Zhao, G.; Li, L.; Tang, Y.; Wu, C.; Wan, C. In-Situ Synthesis of Ultrasmall Au Nanoparticles on Bimetallic Metal-Organic Framework with Enhanced Electrochemical Activity for Estrone Sensing. *Anal. Chim. Acta* **2021**, *1152*, No. 338242.
- (20) Qin, L.; Zeng, G.; Lai, C.; Huang, D.; Xu, P.; Zhang, C.; Cheng, M.; Liu, X.; Liu, S.; Li, B.; Yi, H. “Gold Rush” in Modern Science: Fabrication Strategies and Typical Advanced Applications of Gold Nanoparticles in Sensing. *Coord. Chem. Rev.* **2018**, *359*, 1–31.
- (21) Guo, S.; Wang, E. Synthesis and Electrochemical Applications of Gold Nanoparticles. *Anal. Chim. Acta* **2007**, *598*, 181–192.
- (22) Ma, H.; Yin, B.; Wang, S.; Jiao, Y.; Pan, W.; Huang, S.; Chen, S.; Meng, F. Synthesis of Silver and Gold Nanoparticles by a Novel Electrochemical Method. *ChemPhysChem* **2004**, *5*, 68–75.
- (23) Sakai, N.; Fujiwara, Y.; Arai, M.; Yu, K.; Tatsuma, T. Electrodeposition of Gold Nanoparticles on ITO: Control of Morphology and Plasmon Resonance-Based Absorption and Scattering. *J. Electroanal. Chem.* **2009**, *628*, 7–15.
- (24) Penner, R. M. Mesoscopic Metal Particles and Wires by Electrodeposition. *J. Phys. Chem. B* **2002**, *106*, 3339–3353.
- (25) Ueda, M.; Dietz, H.; Anders, A.; Kneppel, H.; Meixner, A.; Plieth, W. Double-Pulse Technique as an Electrochemical Tool for Controlling the Preparation of Metallic Nanoparticles. *Electrochim. Acta* **2002**, *48*, 377–386.
- (26) Cui, L.; Yliniemi, K.; Vapaavuori, J.; Lundström, M. Recent Developments of Electrodeposition-Redox Replacement in Metal Recovery and Functional Materials: A Review. *Chem. Eng. J.* **2023**, *465*, No. 142737.
- (27) Korolev, I.; Spatharotis, S.; Yliniemi, K.; Wilson, B. P.; Abbott, A. P.; Lundström, M. Mechanism of Selective Gold Extraction from Multi-Metal Chloride Solutions by Electrodeposition-Redox Replacement. *Green Chem.* **2020**, *22*, 3615–3625.
- (28) Choo, W. L.; Jeffrey, M. I. An Electrochemical Study of Copper Cementation of Gold(I) Thiosulfate. *Hydrometallurgy* **2004**, *71*, 351–362.
- (29) Nguyen, H. H.; Tran, T.; Wong, P. L. M. A Kinetic Study of the Cementation of Gold from Cyanide Solutions onto Copper. *Hydrometallurgy* **1997**, *46*, 55–69.
- (30) Kim, E.; Kim, M.; Lee, J.; Pandey, B. D. Selective Recovery of Gold from Waste Mobile Phone PCBs by Hydrometallurgical Process. *J. Hazard. Mater.* **2011**, *198*, 206–215.
- (31) Seisko, S.; Aroma, J.; Lundström, M. Features Affecting the Cupric Chloride Leaching of Gold. *Miner. Eng.* **2019**, *137*, 94–101.
- (32) Thanh, N. T. K.; Maclean, N.; Mahiddine, S. Mechanisms of Nucleation and Growth of Nanoparticles in Solution. *Chem. Rev.* **2014**, *114*, 7610–7630.
- (33) Winand, R. Chloride Hydrometallurgy. *Hydrometallurgy* **1991**, *27*, 285–316.
- (34) Senanayake, G.; Muir, D. M. Speciation and Reduction Potentials of Metal Ions in Concentrated Chloride and Sulfate Solutions Relevant to Processing Base Metal Sulfides. *Metall. Trans. B* **1988**, *19*, 37–45.
- (35) Leopold, M. C.; Black, J. A.; Bowden, E. F. Influence of Gold Topography on Carboxylic Acid Terminated Self-Assembled Monolayers. *Langmuir* **2002**, *18*, 978–980.
- (36) Trasatti, S.; Petrii, O. A. Real Surface Area Measurements in Electrochemistry. *J. Electroanal. Chem.* **1992**, *327*, 353–376.
- (37) Zhao, H.; Chang, J.; Boika, A.; Bard, A. J. Electrochemistry of High Concentration Copper Chloride Complexes. *Anal. Chem.* **2013**, *85*, 7696–7703.
- (38) Meng, Y.; Bard, A. J. Measurement of Temperature-Dependent Stability Constants of Cu(I) and Cu(II) Chloride Complexes by Voltammetry at a Pt Ultramicroelectrode. *Anal. Chem.* **2015**, *87*, 3498–3504.
- (39) Wojnicki, M.; Rudnik, E.; Luty-Blocho, M.; Paclawski, K.; Fitzner, K. Kinetic Studies of Gold(III) Chloride Complex Reduction and Solid Phase Precipitation in Acidic Aqueous System Using Dimethylamine Borane as Reducing Agent. *Hydrometallurgy* **2012**, *127–128*, 43–53.
- (40) Komsysińska, L.; Staikov, G. Electrocrystallization of Au Nanoparticles on Glassy Carbon from HClO<sub>4</sub> Solution Containing [AuCl<sub>4</sub>]<sup>-</sup>. *Electrochim. Acta* **2008**, *54*, 168–172.
- (41) Kasian, O.; Kulyk, N.; Mingers, A.; Zeradjanin, A. R.; Mayrhofer, K. J. J.; Cherevko, S. Electrochemical Dissolution of

Gold in Presence of Chloride and Bromide Traces Studied by On-Line Electrochemical Inductively Coupled Plasma Mass Spectrometry. *Electrochim. Acta* **2016**, *222*, 1056–1063.

(42) Nicol, M. J. The Anodic Behaviour of Gold: Part I — Oxidation in Acidic Solutions. *Gold Bull.* **1980**, *13*, 46–55.

(43) Seisko, S.; Aroma, J.; Lundström, M. Effect of Redox Potential and OCP in Ferric and Cupric Chloride Leaching of Gold. *Hydrometallurgy* **2020**, *195*, No. 105374.

(44) Yoon, S.; Kim, C.; Lee, B.; Lee, J. H. From a Precursor to an Etchant: Spontaneous Inversion of the Role of Au(III) Chloride for One-Pot Synthesis of Smooth and Spherical Gold Nanoparticles. *Nanoscale Adv.* **2019**, *1*, 2157–2161.

(45) Cheng, Y.; Qiu, C.; Ma, H.; Zhang, X.; Gu, X. Unusual Corrosion Process of Gold Nanoplates and the Mechanism Study. *Nanoscale* **2010**, *2*, 685.

(46) Anastas, P.; Warner, J. 12 Principles of Green Chemistry. In *Green Chemistry: Theory and Practice*; Oxford University Press: New York, pp 30.

(47) Kasper, A. C.; Veit, H. M.; García-Gabaldón, M.; Herranz, V. P. Electrochemical Study of Gold Recovery from Ammoniacal Thiosulfate, Simulating the PCBs Leaching of Mobile Phones. *Electrochim. Acta* **2018**, *259*, 500–509.

(48) Brandon, N. P.; Mahmood, M. N.; Page, P. W.; Roberts, C. A. The Direct Electrowinning of Gold from Dilute Cyanide Leach Liquors. *Hydrometallurgy* **1987**, *18*, 305–319.

(49) Barbosa, L. A. D.; Sobral, L. G. S.; Dutra, A. J. B. Gold Electrowinning from Diluted Cyanide Liquors: Performance Evaluation of Different Reaction Systems. *Miner. Eng.* **2001**, *14*, 963–974.

(50) Schlesinger, M. E.; Sole, K. C.; Davenport, W. G.; Alvear Flores, G. R. F. Solvent Extraction. In *Extractive Metallurgy of Copper*; Elsevier, 2022; pp 407–436 DOI: 10.1016/B978-0-12-821875-4.00020-1.

(51) Crundwell, F. K.; Moats, M. S.; Ramachandran, V.; Robinson, T. G.; Davenport, W. G. Hydrometallurgical Production of High-Purity Nickel and Cobalt. In *Extractive Metallurgy of Nickel, Cobalt and Platinum Group Metals*; Elsevier, 2011, pp 281–299 DOI: 10.1016/B978-0-08-096809-4.10023-1.

(52) Soltani, F.; Darabi, H.; Aram, R.; Ghadiri, M. Leaching and Solvent Extraction Purification of Zinc from Mehdiabad Complex Oxide Ore. *Sci. Rep.* **2021**, *11*, No. 1566.

(53) Kim, E.-y.; Kim, M.; Lee, J.; Yoo, K.; Jeong, J. Leaching Behavior of Copper Using Electro-Generated Chlorine in Hydrochloric Acid Solution. *Hydrometallurgy* **2010**, *100*, 95–102.

(54) Mular, A. L.; Halbe, D. N.; Barratt, D. J. In *Configuration of Strip/Electrowinning Circuit*; Mineral Processing Plant Design, Practice, and Control Proceedings; Society for Mining, Metallurgy, and Exploration (SME), 2002, Vol. 1–2; pp 1700–1708.

(55) Krznarić, D.; Goričnik, T. Reactions of Copper on the Au(111) Surface in the Underpotential Deposition Region from Chloride Solutions. *Langmuir* **2001**, *17*, 4347–4351.

(56) Gokcen, D.; Bae, S.-E.; Brankovic, S. R. Kinetics of Metal Deposition via Surface-Limited Redox Replacement Reaction. *ECS Trans.* **2011**, *35*, 11–22.

(57) Guo, L.; Searson, P. C. On the Influence of the Nucleation Overpotential on Island Growth in Electrodeposition. *Electrochim. Acta* **2010**, *55*, 4086–4091.

## Recommended by ACS

### Colloidal Black Gold with Broadband Absorption for Plasmon-Induced Dimerization of 4-Nitrothiophenol and Cross-Linking of Thiolated Diazonium Compound

Radwan M. Sarhan, Yan Lu, *et al.*

MAY 22, 2023

THE JOURNAL OF PHYSICAL CHEMISTRY C

READ 

### Role of the Deep Eutectic Solvent Reline in the Synthesis of Gold Nanoparticles

Sukanya Datta, Laura Torrente-Murciano, *et al.*

JULY 03, 2023

ACS SUSTAINABLE CHEMISTRY & ENGINEERING

READ 

### Capture and Extraction of Gold from Aqueous Solution via the Iron Electrocoagulation Method

Guofu Dai, Chenlong Duan, *et al.*

APRIL 03, 2023

ACS ES&T ENGINEERING

READ 

### Site-Specific Chemistry on Gold Nanorods: Curvature-Guided Surface Dewetting and Supracolloidal Polymerization

Hanyi Duan, Jie He, *et al.*

JUNE 21, 2023

ACS NANO

READ 

Get More Suggestions >